NASA Technical Memorandum 87240

The Predicted Effect of Aerodynamic Detuning on Coupled Bending-Torsion Unstalled Supersonic Flutter

Daniel Hoyniak
Lewis Research Center
Cleveland, Ohio

and

Sanford Fleeter
Purdue University
West Lafayette, Indiana

Prepared for the
31st International Gas Turbine Conference
sponsored by the American Society of Mechanical Engineers
Dusseldorf, West Germany, June 8–12, 1986

NASA

THE PREDICTED EFFECT OF AERODYNAMIC DETUNING ON COUPLED BENDING-TORSION UNSTALLED SUPERSONIC FLUTTER

Daniel Hoyniak
National Aeronautics and Space Administration
Lewis Research Center
Cleveland, Ohio 44135

and

Sanford Fleeter*
Purdue University
West Lafayette, Indiana 47907

SUMMARY

A mathematical model is developed to predict the enhanced coupled bending-torsion unstalled supersonic flutter stability due to alternate circumferential spacing aerodynamic detuning of a turbomachine rotor. The translational and torsional unsteady aerodynamic coefficients are developed in terms of influence coefficients, with the coupled bending-torsion stability analysis developed by considering the coupled equations of motion together with the unsteady aerodynamic loading. The effect of this aerodynamic detuning on coupled bending-torsion unstalled supersonic flutter as well as the verification of the modeling are then demonstrated by considering an unstable 12 bladed rotor, with Verdon's uniformly spaced Cascade B flow geometry as a baseline. It was found that with the elastic axis and center of gravity at or forward of the airfoil midchord, 10 percent aerodynamic detuning results in a lower critical reduced frequency value as compared to the baseline rotor, thereby demonstrating the aerodynamic detuning stability enhancement. However, with the elastic axis and center of gravity at 60 percent of the chord, this type of aerodynamic detuning has a minimal effect on stability. For both uniform and nonuniform circumferentially spaced rotors, a single degree of freedom torsion mode analysis was shown to be appropriate for values of the bending-torsion natural frequency ratio lower than 0.6 and higher than 1.2. However, for values of this natural frequency ratio between 0.6 and 1.2, a coupled flutter stability analysis is required. When the elastic axis and center of gravity are not coincident, the effect of detuning on cascade stability was found to be very sensitive to the location of the center of gravity with respect to the elastic axis. In addition, it was determined that when the center of gravity was forward of an elastic axis located at midchord, a single degree of freedom torsion model did not accurately predict cascade stability.

E-2915

INTRODUCTION

To analyze the aeroelastic stability of gas turbine engine bladed-disk assemblies, a typical airfoil section approach is utilized. Thus, the three-dimensional flow field is approximated by two-dimensional chordwise strips

---

*Professor, School of Mechanical Engineering and Director, Thermal Sciences and Propulsion Center.

along the span of the blade. Also, the rotor is assumed to be tuned, with all of the blades identical and uniformly spaced. Hence, the airfoil structural properties and the unsteady aerodynamic loading at a particular span location are assumed to be identical for each airfoil. However, due to manufacturing tolerances, the individual airfoil natural frequencies are never identical, i.e., the rotors are structurally detuned.

Whitehead (ref. 1) developed an analysis which demonstrated the effects of blade natural frequency structural detuning on the flutter characteristics of a rotor. Several other investigators have shown that the deliberate introduction of structural detuning into a rotor design can be utilized as a passive means of controlling rotor stability, (refs. 2 to 5). Kielb and Kaza (refs. 2 and 3) and Bendiksen and Friedmann (ref. 6) have both demonstrated that the coupling between the bending and the torsion modes of vibration can have a significant effect on the flutter characteristics of a tuned rotor configuration.

Another approach to passive rotor stability control, termed aerodynamic detuning, has recently been proposed (ref. 7). Aerodynamic detuning is defined as designed passage-to-passage variations in the unsteady aerodynamic flow field of the blade row. The subsequent blade-to-blade differences in the unsteady aerodynamic loading result in the blading not responding in a classical traveling wave mode typical of conventional tuned rotor analyses. In reference 7, the effect of aerodynamic detuning on unstalled supersonic single degree of freedom torsion mode flutter, with the aerodynamic detuning accomplished by alternating the circumferential spacing of adjacent rotor blades was considered. The effect of combining both structural and aerodynamic detuning on supersonic unstalled torsional flutter, as well as the forced response characteristics of the single degree of freedom model are reported on in references 8 and 9, respectively.

In this paper, this alternate circumferential spacing aerodynamic detuning torsional model is extended to analyze the unsteady translational unsteady aerodynamics to account for the coupling between the bending and torsion motions of the airfoils. The unsteady aerodynamic loading resulting from both the torsional and the translational motions of the airfoils were developed and presented here in terms of aerodynamic influence coefficients. A coupled bending-torsion unstalled supersonic flutter analysis appropriate for conventional tuned both and aerodynamically and structurally detuned rotors was then developed by considering the coupled equations of motion together with the unsteady aerodynamic loading. While the model is capable of analyzing both types of detuning only the effect of aerodynamic detuning will be addressed in this paper. The enhanced coupled bending-torsion unstalled supersonic flutter stability due to alternate circumferential aerodynamic detuning is then demonstrated by applying this analysis to an unstable 12 bladed rotor, with Verdon's Cascade B flow geometry (ref. 10) as a baseline uniformly spaced geometry. The results are presented herein in terms of the critical reduced frequency, k_f, as a function of the bending-torsion frequency, ω_h/ω_α, for 0 and 10 percent levels of aerodynamic detuning.

NOMENCLATURE

a dimensionless elastic axis offset

b blade semichord, $b = \frac{c}{2}$

C	airfoil chord
c	perturbation in speed of sound
d	blade passage height
$\bar{h}$	complex bending displacement
I	mass moment of inertia
K	linear spring constant
k	reduced frequency, $k = \omega C/U_\infty$
L	unsteady aerodynamic lifting force per unit span
l	dimensionless unsteady aerodynamic lift coefficient
M	unsteady aerodynamic moment per unit span
M_∞	cascade inlet Mach number
m	dimensionless unsteady aerodynamic moment coefficient
r_α	dimensionless radius of gyration
S	airfoil spacing
S_d	gap distance for detuned cascade
S_α	static mass moment per unit span about elastic axis
U_∞	cascade inlet velocity
u	perturbation chordwise velocity
v	perturbation normal velocity
x	dimensionless chordwise coordinate, $x = X/C$
x_α	dimensionless CG-EA offset
y	dimensionless normal coordinate, $y = Y/C$
α	amplitude of torsional displacement
$\bar{\alpha}$	complex torsional displacement
β	interblade phase angle
γ	complex eigenvalue
γ_α	ratio of natural frequency in torsion to the reference frequency
γ_h	ratio of natural frequency in bending to the reference frequency

ε level of detuning

μ mass ratio

ζ structural damping ratio

ω oscillatory frequency

ω_h natural frequency in bending

ω_α natural frequency in torsion

[ ] matrix

Subscripts

d detuned cascade

f critical condition

h refers to bending displacement

R_e reference for the set of even numbered airfoils

R_o reference for the set of odd numbered airfoils

α refers to torsional displacement

UNSTEADY AERODYNAMIC MODEL

The unsteady aerodynamic models utilized in flutter analyses of fan and compressor blading consider a two-dimensional cascade with uniformly spaced airfoils to represent a typical rotor blade section. The motion dependent unsteady aerodynamic loading is determined by harmonically oscillating the airfoils in a classical traveling wave mode, i.e., each airfoil having the same amplitude with a constant interblade phase angle between adjacent airfoils.

For unstalled supersonic flutter, a flat plate airfoil cascade embedded in a supersonic inlet flow field with a subsonic leading edge locus is considered, figure 1. The fluid is assumed to be an inviscid perfect gas with the flow isentropic, adiabatic, and irrotational. The unsteady continuity and Euler equations are linearized by assuming that the unsteady perturbations are small as compared to the uniform through flow. The boundary conditions, applied on the mean positions of the oscillating airfoils, require the flow to be tangent to the airfoil surfaces.

Several investigators have utilized various techniques to predict the unsteady aerodynamics associated with the torsional and translational motions of the airfoil cascade depicted in figure 1. Of particular interest are the analyses of Verdon (ref. 11), Brix and Platzer (ref. 12), and Caruthers (ref. 13). These utilize a finite cascade representation of the semi-infinite cascade, with the cascade periodicity condition enforced by stacking sufficient numbers of uniformly spaced single airfoils until convergence in the unsteady flow field is achieved. An analogous finite cascade model is utilized for the

alternate circumferentially spaced aerodynamically detuned cascade, figure 2. As seen, for this detuned cascade configuration, there are two sets of airfoils, for convenience termed the set of even numbered airfoils and the set of odd numbered airfoils. Thus, convergence in the detuned unsteady flow field is achieved by stacking sufficient numbers of two airfoils at a time. The level of detuning introduced into the cascade is specified by the parameter, ϵ. This quantity is the amount by which the passage height d given in figure 1 is reduced in order to obtain the detuned passage height d_1, shown in figure 2.

The formulation of the linearized differential equations describing the unsteady perturbation quantities for a finite aerodynamically detuned cascade is based on the method of characteristics analysis developed by Brix and Platzer for the finite uniformly spaced cascade (ref. 12). The independent variables are the dimensionless chordwise and normal coordinates, x and y. The dependent variables are the chordwise, normal, and sonic perturbation velocities, u, v, and c, respectively. Assuming harmonic motion, the linearized differential equations describing the unsteady perturbation flow field are specified in equation (1).

$$\frac{\partial u}{\partial x} + \sqrt{M_\infty^2 - 1}\,\frac{\partial v}{\partial y} + \frac{\partial c}{\partial x} + ikM_\infty^2 c = 0 \tag{1a}$$

$$\frac{\partial u}{\partial x} + \frac{\partial c}{\partial x} + iku = 0 \tag{1b}$$

$$\frac{\partial u}{\partial x} - \sqrt{M_\infty^2 - 1}\,\frac{\partial v}{\partial x} = 0 \tag{1c}$$

The flow tangency boundary condition requires that the normal perturbation velocity component, v, be equal to the normal velocity of the oscillating airfoils, and is applied at the mean airfoil positions. For the aerodynamically tuned airfoil cascade executing both harmonic translational (bending) and torsional motions, the dimensionless normal perturbation velocity component on the n-th airfoil is specified in equation (2).

$$v_n(x,y_s,t) = \left\{\frac{h_o}{C}\,ik - \alpha_o[1 + (x - x_o)\,ik]\right\} e^{i(kt+n\beta)} \tag{2}$$

where h_o and α_o denote the translational and torsional amplitudes of a reference airfoil; β is the interblade phase angle; and x_o, y_s, and k are the elastic axis location as measured from the airfoil leading edge, the mean position of the airfoil, and the reduced frequency, respectively.

The unsteady perturbation pressure distributions on the two reference airfoils, one for the set of even numbered airfoils and the other for the set of odd numbered airfoils, R_e and R_o, are determined from the perturbation velocities by the unsteady Bernoulli equation. The unsteady aerodynamic lift and moment on these reference airfoils are then calculated by integrating the unsteady perturbation pressure differences across their chord lines, equation (3).

$$L_{R_e,R_o} = \int_0^1 \Delta p(x,y_s,t)dx \tag{3a}$$

$$M_{R_e,R_o} = \int_0^1 (x - x_o)\, \Delta p(x,y_s,t)dx \tag{3a}$$

The double subscript is a shorthand equation notation, with the subscript R_e denoting the equation for the reference airfoil of the set of even numbered airfoils, and R_o the equation for the reference airfoil of the set of odd numbered airfoils.

When the boundary conditions specified in equation (2) are applied to an aerodynamically detuned cascade, the alternate circumferentially spaced airfoils are required to oscillate with an equal amplitude and a constant interblade phase angle, a situation not appropriate for the detuned cascade. In addition, the application of this analysis is unduly costly because the complete periodic perturbation flow field must be recalculated, not only for every new cascade geometry and flow condition, but also for each interblade phase angle for a particular cascade geometry and flow field.

These restrictions can be eliminated by using the aerodynamic influence coefficient technique introduced in reference 7. A complete derivation of the influence coefficients required to describe the unsteady aerodynamic moments resulting from harmonic torsional motion of the airfoils in an alternate circumferentially spaced detuned cascade is presented in this reference. The required unsteady aerodynamic translational lift coefficients are obtained in an analogous manner, with this derivation not repeated herein.

The unsteady aerodynamic lift and moment on the two reference airfoils of an alternate circumferentially spaced detuned cascade undergoing both harmonic torsional and translational motions are defined in terms of influence coefficients in equation (4).

$$L_{R_e,R_o} = -\pi\rho b^3\omega^2 \left\{ \left(\frac{h_{R_e}}{b}\right) \left[l_h^e\right]_{R_e,R_o} + \left(\frac{h_{R_o}}{b}\right) \left[l_h^o\right]_{R_e,R_o} + \alpha_{R_e} \left[l_\alpha^e\right]_{R_e,R_o} + \alpha_{R_o} \left[l_\alpha^o\right]_{R_e,R_o} \right\} e^{i\omega t} \tag{4a}$$

$$M_{R_e,R_o} = \pi\rho b^4\omega^2 \left\{ \left(\frac{h_{R_e}}{b}\right) \left[m_h^e\right]_{R_e,R_o} + \left(\frac{h_{R_o}}{b}\right) \left[m_h^o\right]_{R_e,R_o} + \alpha_{R_e} \left[m_\alpha^e\right]_{R_e,R_o} + \alpha_{R_o} \left[m_\alpha^o\right]_{R_e,R_o} \right\} e^{i\omega t} \tag{4b}$$

The superscripts e and o refer to the sets of even numbered and odd numbered airfoils, respectively. The negative sign in equation (4a) indicates that for a positive downward translational displacement, the lift is negative, and thus acts in an upward direction.

The term $\left[l_h^e\right]_{R_e,R_o}$ is the nondimensional unsteady lift per unit translational displacement on the reference airfoil R_e or R_o due to unit amplitude translational displacement of all of the even numbered airfoils with the odd numbered airfoils fixed. $\left[l_h^o\right]_{R_e,R_o}$ is the corresponding lift on the reference airfoils due to unit amplitude translational displacements of all of the odd numbered airfoils with the even numbered airfoils fixed. Similarly, $\left[l_\alpha^e\right]_{R_e,R_o}$ is the unsteady lift per unit torsional displacement developed on the two reference airfoils due to unit amplitude torsional motions of the set of even numbered airfoils while the set of odd numbered airfoils is fixed. The unsteady aerodynamic moments on the reference airfoils, $\left[m_h^e\right]_{R_e,R_o}$, $\left[m_h^o\right]_{R_e,R_o}$, $\left[m_\alpha^e\right]_{R_e,R_o}$, $\left[m_\alpha^o\right]_{R_e,R_o}$, are defined in an analogous manner.

The relation between the unsteady aerodynamic lift and moment coefficients specified in equation (4) and those utilized by Kaza and Kielb (ref. 2) for a uniformly spaced cascade, l_{hh}, $l_{h\alpha}$, $l_{\alpha h}$, and $l_{\alpha\alpha}$, are readily obtained, equation (5).

$$l_{hh} = \left[l_h^e\right]_{R_e} + \left(\frac{h_{R_o}}{h_{R_e}}\right)\left[l_h^o\right]_{R_e} \tag{5a}$$

$$l_{h\alpha} = \left[l_\alpha^e\right]_{R_e} + \left(\frac{h_{R_o}}{h_{R_e}}\right)\left[l_\alpha^o\right]_{R_e} \tag{5b}$$

$$l_{\alpha h} = \left[m_h^e\right]_{R_e} + \left(\frac{\alpha_{R_o}}{\alpha_{R_e}}\right)\left[m_h^o\right]_{R_e} \tag{5c}$$

$$l_{\alpha\alpha} = \left[m_\alpha^e\right]_{R_e} + \left(\frac{\alpha_{R_o}}{\alpha_{R_e}}\right)\left[m_\alpha^o\right]_{R_e} \tag{5d}$$

Similar expressions can also be obtained in terms of the reference airfoil for the set of odd numbered airfoils, R_o.

EQUATIONS OF MOTION

The equations of motion for both conventional uniform and alternate circumferentially spaced aerodynamically detuned cascade configurations are developed by considering the typical airfoil sections depicted schematically in figure 3. Translational displacements of the reference airfoils, h_{R_e} and h_{R_o}, are defined as positive in the downward direction. Torsional motions of reference airfoils, α_{R_e}, and α_{R_o}, are defined as positive with the leading edge up. The unsteady aerodynamic lift and moment were defined in equation (4) such that a positive lift is upward and a positive moment is leading edge up.

The inertia and stiffness properties of the airfoil section are modeled by the mass moment of inertia about the elastic axis and by linear springs attached at the elastic axis. Applying Lagrange's technique, the following differential equations of motion for the two reference airfoils of the detuned cascade are obtained.

$$\begin{aligned} m_{R_e,R_o}\,\ddot{\vec{h}}_{R_e,R_o} + S_{\alpha_{R_e,R_o}}\,\ddot{\vec{\alpha}}_{R_e,R_o} + \left(1 + 2i\zeta_{h_{R_e,R_o}}\right) m_{R_e,R_o}\,\omega^2_{h_{R_e,R_o}}\,\vec{h}_{R_e,R_o} &= -L_{R_e,R_o} \\ S_{\alpha_{R_e,R_o}}\,\ddot{\vec{h}}_{R_e,R_o} + I_{\alpha_{R_e,R_o}}\,\ddot{\vec{\alpha}}_{R_e,R_o} + \left(1 + 2i\zeta_{\alpha_{R_e,R_o}}\right) I_{\alpha_{R_e,R_o}}\,\omega^2_{\alpha_{R_e,R_o}}\,\vec{\alpha}_{R_e,R_o} &= M_{R_e,R_o} \end{aligned} \tag{6}$$

where the damping ratios for both translation and torsional motions are denoted by $\zeta_{h_{R_e,R_o}}$, and $\zeta_{\alpha_{R_e,R_o}}$, and the undamped natural frequencies are

$$\omega_{h_{R_e,R_o}} = \sqrt{K_{h_{R_e,R_o}}/m_{R_e,R_o}} \quad \text{and} \quad \omega_{\alpha_{R_e,R_o}} = \sqrt{K_{\alpha_{R_e,R_o}}/I_{\alpha_{R_e,R_o}}}\,.$$

For harmonic motions of the airfoils, the differential equations of motion, equation (6), can be written as an eigenvalue problem from which the stability of the conventional and the aerodynamically detuned cascade configurations can be determined. This eigenvalue problem is specified in matrix form in equation (7).

$$\begin{bmatrix} \mu_{h_1} & \left[l_h^o\right]_{R_e} & \mu_{h_3} & \left[l_\alpha^o\right]_{R_e} \\ \left[l_h^e\right]_{R_o} & \mu_{h_2} & \left[l_h^e\right]_{R_o} & \mu_{h_4} \\ \mu_{\alpha_1} & \left[m_h^o\right]_{R_e} & \mu_{\alpha_2} & \left[m_\alpha^o\right]_{R_e} \\ \left[m_h^e\right]_{R_o} & \mu_{\alpha_3} & \left[m_\alpha^e\right]_{R_o} & \mu_{\alpha_4} \end{bmatrix} \begin{Bmatrix} \frac{h_{R_e}}{b} \\ \frac{h_{R_o}}{b} \\ \alpha_{R_e} \\ \alpha_{R_o} \end{Bmatrix} = \{0\} \qquad (7)$$

where

$$\mu_{h_1} = \mu_{R_e} + \left[l_h^e\right]_{R_e} - \left(1 + 2i\zeta_{h_{R_e}}\right) \mu_{R_e} \gamma_{h_{R_e}}^2 \gamma$$

$$\mu_{h_2} = \mu_{R_o} + \left[l_h^o\right]_{R_e} - \left(1 + 2i\zeta_{h_{R_o}}\right) \mu_{R_o} \gamma_{h_{R_o}}^2 \gamma$$

$$\mu_{h_3} = \mu_{R_e} x_{\alpha_{R_e}} + \left[l_\alpha^e\right]_{R_e}$$

$$\mu_{h_4} = \mu_{R_o} x_{\alpha_{R_o}} + \left[l_\alpha^o\right]_{R_o}$$

$$\mu_{\alpha_2} = \mu_{R_e} r_{\alpha_{R_e}}^2 + \left[m_\alpha^e\right]_{R_e} - \left(1 + 2i\zeta_{\alpha_{R_e}}\right) \mu_{R_e} r_{\alpha_{R_e}}^2 \gamma_{\alpha_{R_e}}^2 \gamma$$

$$\mu_{\alpha_4} = \mu_{R_o} r_{\alpha_{R_o}}^2 + \left[m_\alpha^o\right]_{R_o} - \left(1 + 2i\zeta_{\alpha_{R_o}}\right) \mu_{R_e} r_{\alpha_{R_o}}^2 \gamma_{\alpha_{R_o}}^2 \gamma$$

$$\mu_{a_1} = \mu_{R_e} x_{\alpha_{R_e}} + \left[m_h^e\right]_{R_e}$$

$$\mu_{a_3} = \mu_{R_o} x_{\alpha_{R_o}} + \left[m_h^o\right]_{R_o}$$

$$\mu_{R_e,R_o} = \frac{m_{R_e,R_o}}{\pi\rho b^2} \; ; \qquad r_{\alpha_{R_e,R_o}}^2 = \frac{I_{\alpha_{R_e,R_o}}}{m_{R_e,R_o} b^2}$$

$$\gamma_{h_{R_e,R_o}} = \frac{\omega_{h_{R_e,R_o}}}{\omega_o} \; ; \quad \gamma_{\alpha_{R_e,R_o}} = \frac{\omega_{\alpha_{R_e,R_o}}}{\omega_o}$$

$$x_{\alpha_{R_e,R_o}} = \frac{S_{\alpha_{R_e,R_o}}}{M_{R_e,R_o} b} \; ; \quad \omega_o = \text{reference frequency}$$

$$\gamma = \left(\frac{\omega_o}{\omega}\right)^2$$

The stability of the cascade configuration is obtained by solving equation (7) and then relating the complex eigenvalue γ to the complex frequency ratio as shown below.

$$\frac{\omega}{\omega_o} = \frac{1}{\sqrt{\gamma}} \tag{8}$$

The eigenvalues obtained from equation (7) are complex. Therefore, the stability of the system is determined by the sign of the real part of (ω/ω_o) in equation (8). When the real part of (ω/ω_o) is negative, the amplitude of the harmonic motion of the airfoil will decay, indicating a stable casade configuration. A positive sign for the real part of (ω/ω_o) indicates that the airfoil motion will increase in amplitude and that the cascade is unstable. A value of zero indicates that the cascade is neutrally stable. The imaginary part of (ω/ω_o) specifies the ratio of the flutter frequency, ω, to the reference frequency, ω_o.

RESULTS

To demonstrate the stability enhancement due to alternate circumferential blade spacing aerodynamic detuning on unstalled supersonic coupled bending-torsion flutter, an unstable baseline uniformly spaced 12 bladed rotor based on Verdon's Cascade B is considered. This baseline rotor is also utilized to verify the validity and the formulation of this mathematical model. The baseline uniform circumferentially spaced Cascade B flow geometry is schematically depicted in figure 4, and is characterized by a stagger angle of 63.4°, a solidity of 1.497, and an inlet Mach number of 1.281.

The validity of both the aerodynamic influence coefficient formulation and the translational and torsional unsteady aerodynamic finite cascade model are verified by comparing predictions for the translational and torsional unsteady aerodynamic coefficient, l_{hh} and $l_{\alpha\alpha}$, from the model developed herein with corresponding predictions from the infinite cascade analysis of Adamczyk and Goldstein (ref. 14) for a uniformly spaced baseline Cascade B flow geometry at a unity reduced frequency. As seen in figures 5 and 6, there is excellent agreement for both coefficients between the two techniques.

The formulation of the coupled bending-torsion eigenvalue problem is verified by comparing the coupled stability predictions from the model developed by Bendiksen and Friedmann for a uniformly spaced cascade (ref. 6) with corresponding predictions from the model developed herein. For this verification, the baseline Cascade B rotor is considered with a midchord elastic axis location, a center of gravity specified by $x_\alpha = 0.1$, and a damping ratio of $\zeta = 0.0025$. Figure 7 presents the results of this correlation in the format of the critical reduced frequency versus the bending-torsion natural frequency ratio. The good agreement between these two models is apparent.

With the validity and formulation of this mathematical model verified, attention is now turned to utilizing this model to consider the stability enhancement due to alternate circumferential blade spacing aerodynamic detuning on unstalled supersonic coupled bending-torsion flutter. This is accomplished by utilizing an unstable baseline uniformly spaced 12 bladed rotor based on Verdon's Cascade B flow geometry as well as an alternate circumferentially spaced rotor with 10 percent aerodynamic detuning. The flow geometries for these uniformly spaced and nonuniformly spaced cases are schematically depicted in figure 8.

The stability of a given rotor design is predicted by the eigenvalue problem specified in equation (7). Typical bending and torsion mode root locus plots are presented in figures 9 and 10, respectively, for the baseline Cascade B 12 bladed rotor at a reduced frequency of 1.0. These were determined from equation (7) by considering a value of 0.1 for the bending-torsion natural frequency ratio. Figure 9 shows that the bending modes are all stable. However, as seen in figure 10, the torsion modes are unstable for forward traveling waves characterized by interblade phase angles between 30 and 150°.

The coupled bending-torsion stability results for both the baseline uniformly spaced and the 10 percent alternate circumferential aerodynamically detuned rotors are presented in figure 11 in the format of the critical reduced frequency as a function of the bending-torsion natural frequency ratio. For both cascades, the elastic axis and the center of gravity are coincident at the blade midchord. Also indicated are the single degree of freedom torsion mode results for both cascades. It should be noted that with the elastic axis and the center of gravity coincident, the equations of motion are coupled only through the unsteady aerodynamic loading terms.

As seen in figure 11, the aerodynamically detuned rotor has a lower critical reduced frequency value than does the baseline tuned rotor, thereby demonstrating the stability enhancement due to aerodynamic detuning. Also, both the tuned and the detuned cascades behave like their single degree of freedom torsion mode counterparts for values of the bending-torsion natural frequency ratio lower than 0.6 and >1.2. This indicates that the bending mode is not coupling with the torsion mode at the higher natural frequency ratios for these cascade configurations. However, for values of this ratio >0.6 and <1.2, coupling effects are significant. It is interesting to note that as shown in figure 11 the difference between the tuned and detuned curves for the coupled bending torsion model is about the same as indicated for the single degree of freedom results. Thus the effect of aerodynamic detuning seems to be independent of the bonding-torsion frequency ratio.

For coupled bending-torsion stability, the locations of the elastic axis and the center of gravity are significant. Figures 12 and 13 show the effect

of moving the elastic axis and the center of gravity forward and aft of midchord, respectively, on the stability of both the baseline and 10 percent circumferential aerodynamically detuned rotors.

With the elastic axis and the center of gravity located at 40 percent of the chord (a = -0.1), figure 12 shows the stability enhancement due to aerodynamic detuning, with the alternate circumferentially spaced rotor more stable than the uniformly spaced baseline rotor. Also, for values of the bending-torsion natural frequency ratio lower than 0.6 and higher than 1.2, the stability of both the baseline and the detuned rotors are predicted by the single degree of freedom torsion mode results. Again, this indicates that the bending mode is not coupling with the torsion mode at the higher natural frequency ratios. However, coupling between the bending and the torsion modes for both the baseline and the detuned rotors is seen to be significant for values of the natural frequency ratio between 0.6 and 1.2.

With the elastic axis and the center of gravity shifted aft to 60 percent of the chord (a = 0.1), figure 13 shows that circumferential aerodynamic detuning has minimal effect on the critical reduced frequency value. Also, a single degree of freedom torsion mode stability analysis is again seen to be appropriate for values of the bending-torsion natural frequency ratio lower than 0.6 and higher than 1.2. For values of this ratio between 0.6 and 1.2, a coupled stability analysis is required.

The effect of circumferential aerodynamic detuning on cascade stability when the center of gravity is located aft of the elastic axis (x_α = 0.1) is shown in figure 14. This figure indicates that for values of the frequency ratio >1.0, the circumferential aerodynamic has a very beneficial effect on cascade stability. However, for frequency ratio's <1.0, detuning has little effect on the critical reduced frequency. The flutter modes associated with each of the values of reduced frequency of figure 14 are listed in table 1. For values of the bending-torsion frequency ratio <0.40 and >1.60, the coupling between the bending and torsion modes is small and the flutter behavior of both the tuned and detuned cascades can be predicted reasonably well by a single degree of freedom torsion model which utilizes a midchord location for both the elastic axis and center of gravity.

When the center of gravity is located forward of the elastic axis (x_α = -0.1), the behavior of the critical reduced frequency as a function of the bending-torsion frequency ratio is presented in figure 15. In this case, the circumferential aerodynamic detuning has a beneficial effect on cascade stability for values of the frequency ratio lower than 1.0, but very little effect when the frequency ratio is above 1.0. Table I gives the flutter modes associated with the values of the reduced frequency shown in figure 15. With this value of x_α, the coupling between the bending and torsion modes is such that even for low values of the bending-torsion frequency ratio, a single degree of freedom torsion model with the center of gravity and elastic axis coincident at midchord should not be utilized to predict the flutter behavior.

CONCLUSIONS

A model to demonstrate the enhanced coupled bending-torsion unstalled supersonic flutter due to alternate circumferential blade spacing aerodynamic detuning has been developed. This is a finite cascade model, with periodicity

achieved by stacking two airfoils at a time. Also, the translational and torsional unsteady aerodynamic lift and moment coefficients were developed in terms of aerodynamic influence coefficients in a manner that enables both a conventional uniform circumferentially spaced rotor as well as an alternate circumferentially space aerodynamically detuned rotor to be analyzed. The coupled bending-torsion stability analysis was then developed by considering the coupled equations of motion together with the unsteady aerodynamic loading.

The effect of alternate circumferential spacing aerodynamic detuning on coupled bending-torsion unstalled supersonic flutter as well as the verification of the modeling and formulation were demonstrated by applying this analysis to an unstable 12 bladed rotor, with Verdon's Cascade B flow geometry as a baseline uniformly spaced geometry.

With the elastic axis and the center of gravity at or forward of midchord, it was shown that 10 percent alternate circumferential spacing aerodynamic detuning results in a lower critical reduced frequency value than does the baseline tuned rotor over the complete range of bending-torsion natural frequency ratios, thereby demonstrating the stability enhancement due to aerodynamic detuning. However, with the elastic axis and the center of gravity at the 60 percent chord location, the circumferential aerodynamic detuning had a minimal effect on the critical reduced frequency. Also, it was shown that for both the uniform and nonuniform circumferentially spaced rotors, a single degree of freedom flutter torsion mode analysis was appropriate for values of the bending-torsion natural frequency ratio lower than 0.6 and higher than 1.2, indicating that the bending mode does not couple with the torsion mode at the higher values of the bending-torsion natural frequency ratio. However, for values of this natural frequency ratio between 0.6 and 1.2, a coupled flutter stability analysis is required.

When the elastic axis and center of gravity are not coincident, the effect of circumferential aerodynamic detuning on cascade stability was found to be highly dependent on the position of the center of gravity with respect to the elastic axis. When the center of gravity is forward of an elastic axis located at midchord, the introduction of aerodynamic detuning had a beneficial effect for bending-torsion frequency ratios below 1.0. However, detuning had very little effect when the frequency ratio was above 1.0. Moving the center of gravity aft of a midchord elastic axis had the opposite effect. In this case aerodynamic detuning was shown to have a beneficial effect when the frequency ratio was above 1.0, and very little effect for frequency ratios below 1.0. In addition, when the center of gravity was forward of the elastic axis, the coupling between the bending and torsion modes was such that a single degree of freedom torsion analysis which utilized a center of gravity and elastic axis coincident at midchord did not yield accurate stability prediction. This condition was found to be true even for low values of the bending-torsion frequency ratio.

REFERENCES

1. Whitehead, D.S., "Torsional Flutter of Unstalled Cascade Blades at Zero Deflection," Aeronautical Research Council, RəM 3429, Mar. 1964.

2. Kaza, K.R.V. and Kielb, R.E., "Flutter and Response of a Mistuned Cascade in Incompressible Flow", AIAA Journal, Vol. 20, No. 8, Aug. 1982, pp. 1120-1127.

3. Kielb, R.E. and Kaza, K.R.V., "Aeroelastic characteristics of a Cascade of Mistuned Blades in Subsonic and Supersonic Flows," Journal of Vibration, Stress and Reliability in Design, Vol. 105, No. 4, Oct. 1983. pp. 425-433.

4. Bendiksen, O.O., "Flutter of Mistuned Turbomachinery Rotors," ASME Paper No. 83-GT-153, Mar. 1983.

5. Crawley, E.F. and Hall, K.C., "Optimization and Mechanisms of Mistuning in Cascades," ASME Paper 84-GT-196, June, 1984.

6. Bendiksen, O.O. and Friedmann, P.P., "The Effect of Bending-Torsion Coupling on Fan and Compressor Blade Flutter," ASME Paper 81-GT-163, Mar. 1981.

7. Hoyniak, D. and Fleeter, S., "Aerodynamic Detuning Analysis of an Unstalled Supersonic Turbofan Cascade," ASME Paper 85-GT-192, Mar. 1985.

8. Hoyniak, D. and Fleeter, S. "The Effect of Aerodynamic and Structural Detuning on Turbomachine Supersonic Unstalled Torsional Flutter," Structures, Structural Dynamics, and Materials Conference, 26th, AIAA, New York, 1985, pp. 500-514.

9. Hoyniak, D. and Fleeter, S. "Forced Response Analysis of an Aerodynamically Detuned Supersonic Turbomachine Rotor," NASA TM-87093, 1985.

10. Verdon, J.M. and McCune, J.E., "Unsteady Supersonic Cascade in Subsonic Axial Flow," AIAA Journal, Vol. 13, No. 2, Feb. 1975. pp. 193-201.

11. Verdon, J.M., "The Unsteday Aerodynamics of a Finite Supersonic Cascade with Subsonic Axial Flow," Journal of Applied Mechanics, Vol. 40, No. 3, Sept. 1973, pp. 667-671.

12. Brix, C. W. and Platzer, M.F., "Theoretical Investigation of Supersonic Flow Past Oscillating Cascades with Subsonic Leading Edge Locus," AIAA Paper 74-15, Jan. 1974.

13. Caruthers, J.E. and Riffel, R.E., "Aerodynamic Analysis of Supersonic Cascade Vibrating in a Complex Mode," Journal of Sound and Vibration, Vol. 71, No. 2, July 22, 1980, pp. 171-183.

14. Adamczyk, J.J. and Goldstein, M.E., "Unsteady Flow in a Supersonic Cascade with Subsonic Leading Edge Locus," AIAA Journal. Vol. 16, No. 12, Dec. 1978, pp. 1248-1254.

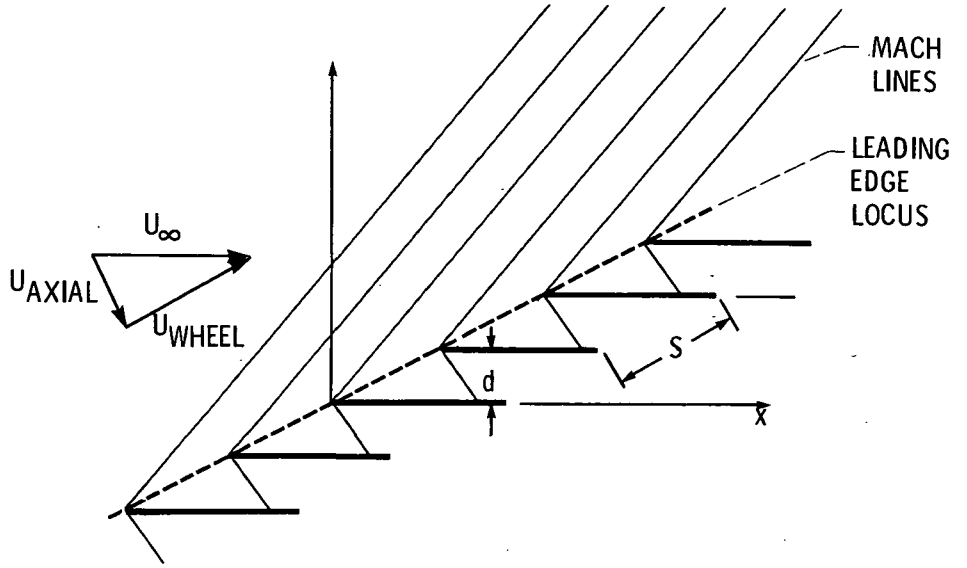

Figure 1. - Uniformly spaced tuned cascade in a supersonic inlet flow field with a subsonic leading edge locus.

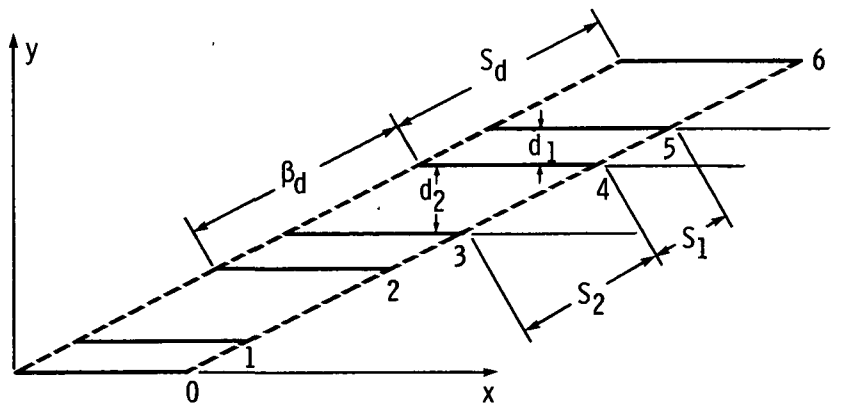

Figure 2. - Finite cascade representation for alternate non-uniform circumferentially spaced cascade.

TABLE I. - FLUTTER MODES FOR CASES WHERE ELASTIC AXIS IS AT MIDCHORD AND $X_\alpha = \pm 0.1$

(a) $x_\alpha = 0.1$; $a = 0.0$; $\zeta = 0.0025$; $\mu = 200$; $r_\alpha = 0.5774$.

W_h/W_α	k_F	Mode	w_h/w_α	k_α	Mode
ϵ = 0 percent			ϵ = 10 percent		
0.1	1.10	Torsion	0.1	1.100	Torsion
.2	(Not run)	(Not run)	.2	(Not run)	(Not run)
.4	1.100	Torsion	.4	1.085	Torsion
.6	1.085	Torsion	.6	1.080	Torsion
.7	1.060	Torsion	.7	(Not run)	(Not run)
.8	1.080	Bending	.8	1.080	Bending
.9	1.230	Bending	.9	1.230	Bending
1.0	1.280	Torsion	1.0	1.255	Torsion
1.1	1.235	↓	1.1	(Not run)	(Not run)
1.2	1.210		1.2	1.175	Torsion
1.4	1.190		1.4	1.145	↓
1.6	1.175		1.6	1.150	
1.8	1.170	↓	1.8	1.135	↓

(b) $x_\alpha = -0.1$; $a = 0.0$; $\zeta = 0.0025$; $\mu = 200$; $r_\alpha = 0.5774$.

W_h/W_α	k_F	Mode	w_h/w_α	k_α	Mode
ϵ = 0 percent			ϵ = 10 percent		
0.1	1.200	Torsion	0.1	1.175	Torsion
.2	(Not run)	(Not run)	.2	(Not run)	(Not run)
.4	1.210	Torsion	.4	1.175	Torsion
.6	1.225	Torsion	.6	1.200	Torsion
.7	(Not run)	(Not run)	.7	(Not run)	(Not run)
.8	1.270	Torsion	.8	1.230	Torsion
.9	1.285	↓	.9	1.230	↓
1.0	1.300		1.0	1.285	
1.1	1.2660	↓	1.1	1.245	↓
1.2	1.200	Bending	1.2	1.195	Bending
1.4	1.120	Bending	1.4	1.112	Bending
1.6	1.100	Torsion	1.6	1.090	Torsion
1.8	1.110	Torsion	1.8	1.10	Torsion

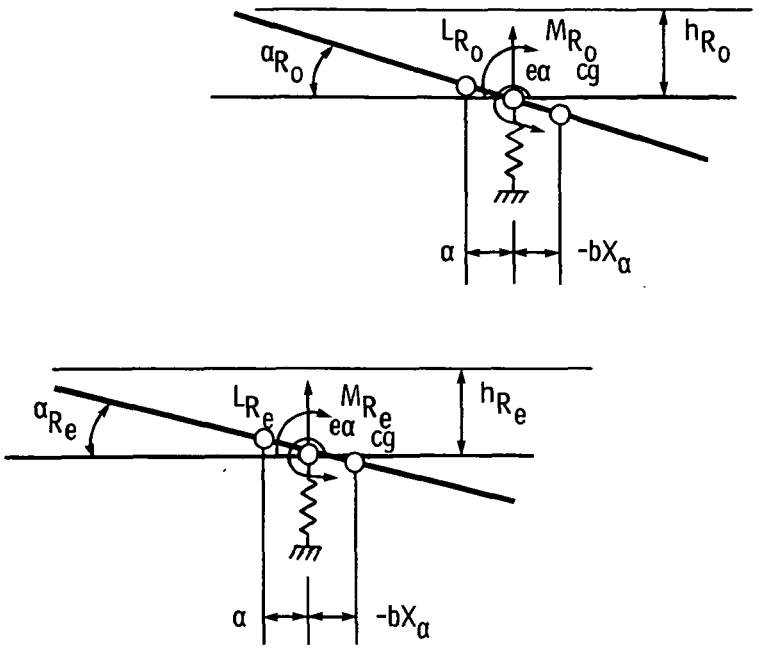

Figure 3. - Coupled bending-orsion model of typical blade sections in a circumferentially detuned cascade.

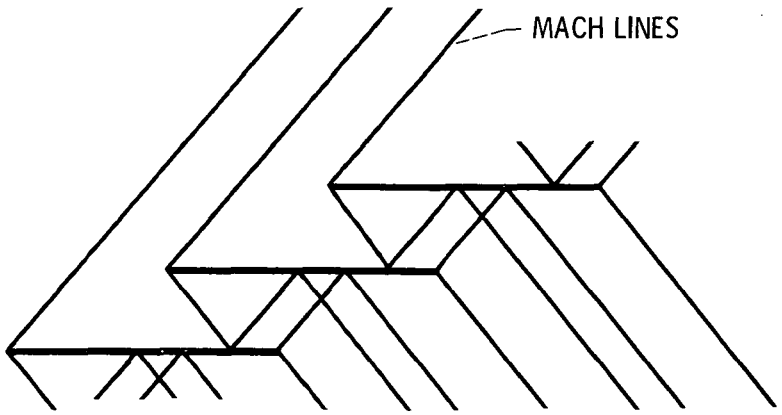

Figure 4. - Baseline cascade B uniformly spaced flow geometry.

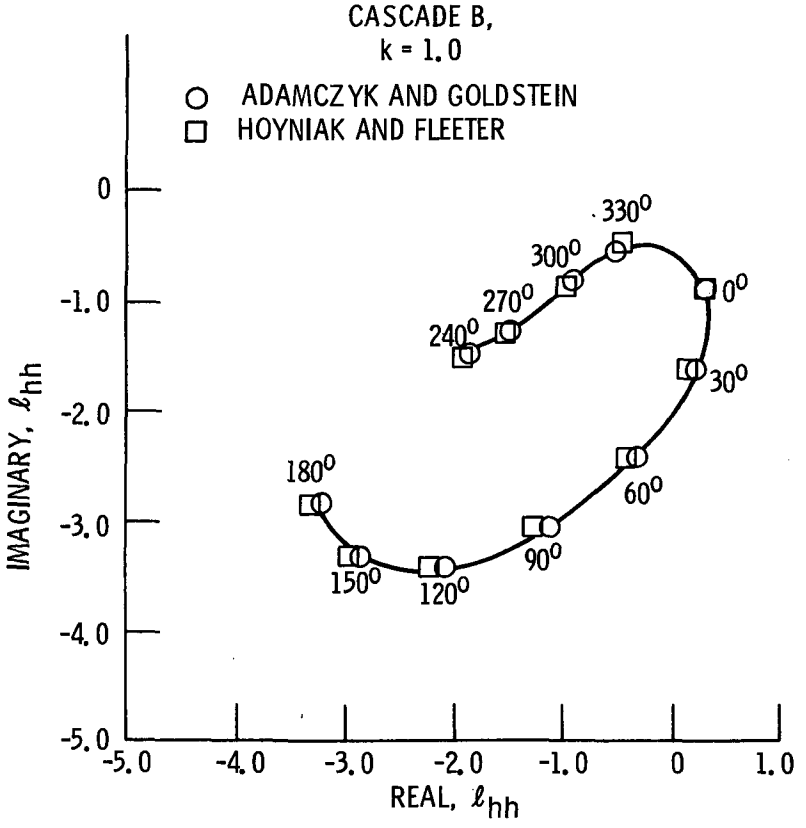

Figure 5. - Unsteady lift coefficient, ℓ_{hh} for Cascade B.

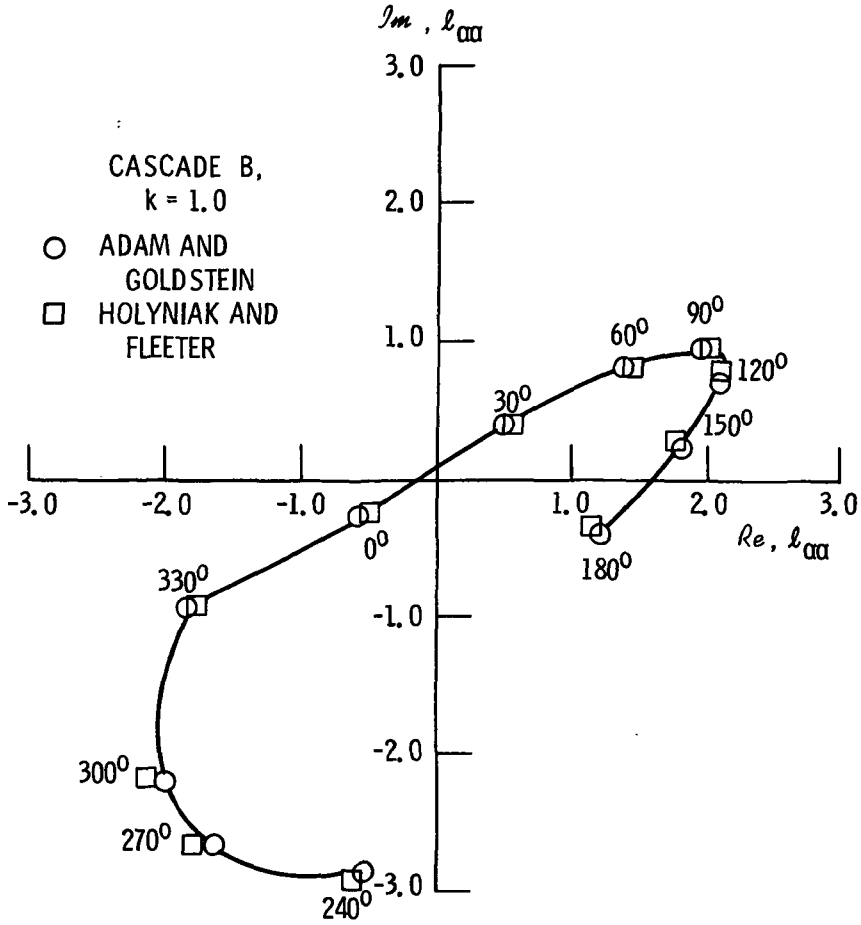

Figure 6. - Unsteady moment coefficent, $1_{\alpha\alpha}$, for Cascade B.

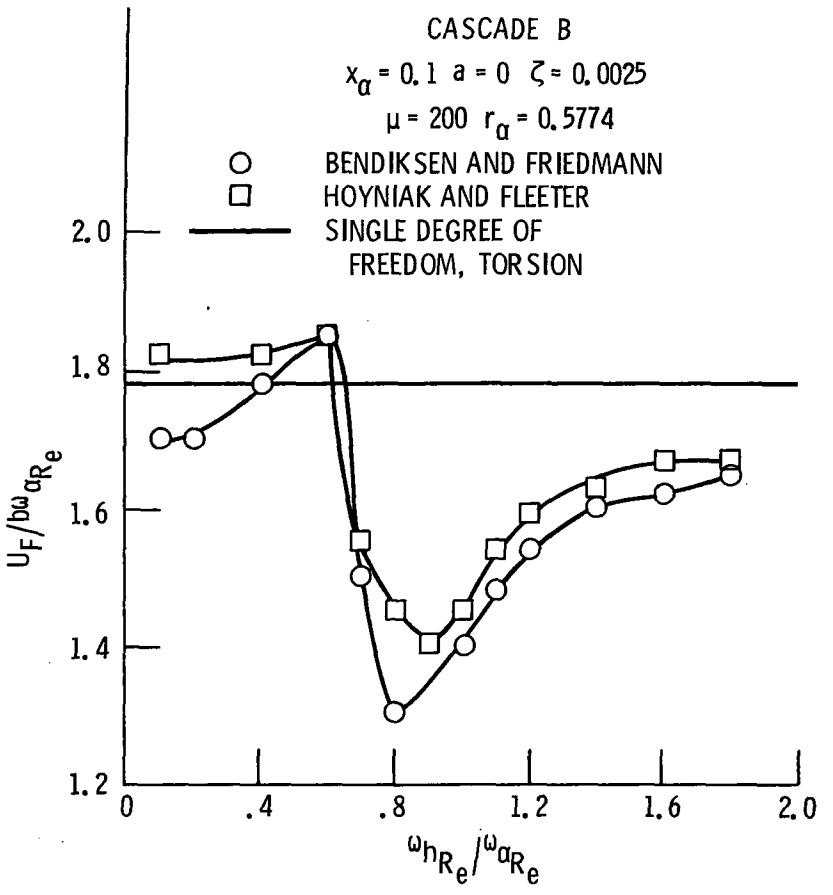

Figure 7. - Verification of the coupled bending-torsion eigenvalue model.

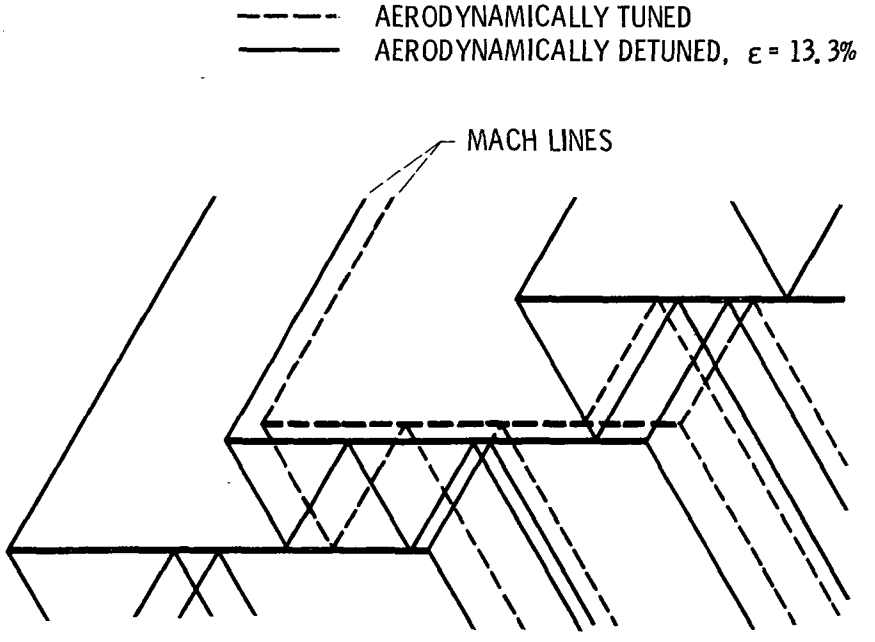

Figure 8. - The flow geometries of the baseline and circumferentially detuned cascades.

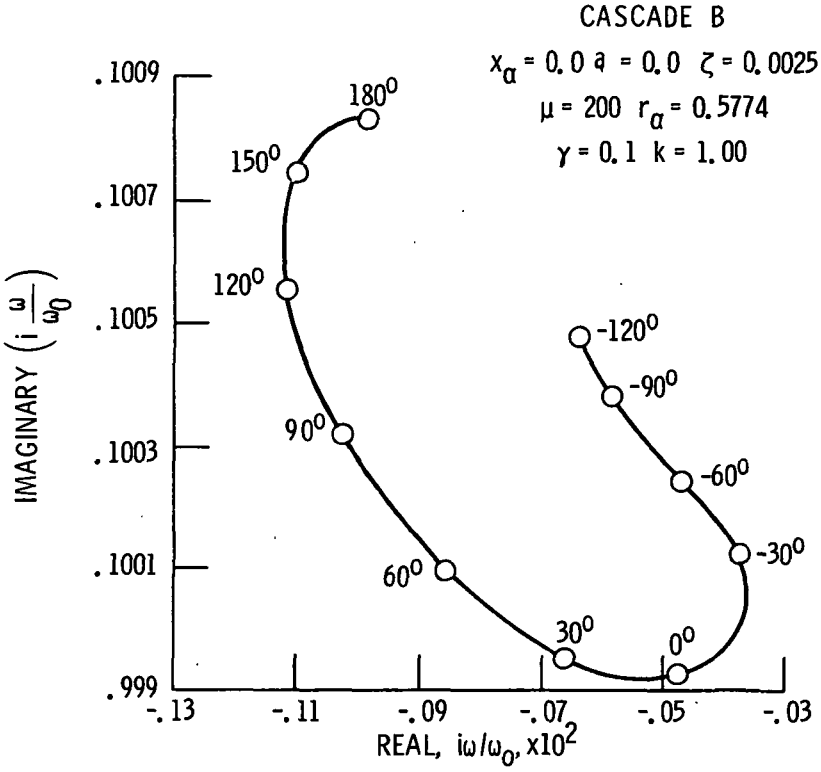

Figure 9. - Bending mode root locus plot for a twelve bladed rotor.

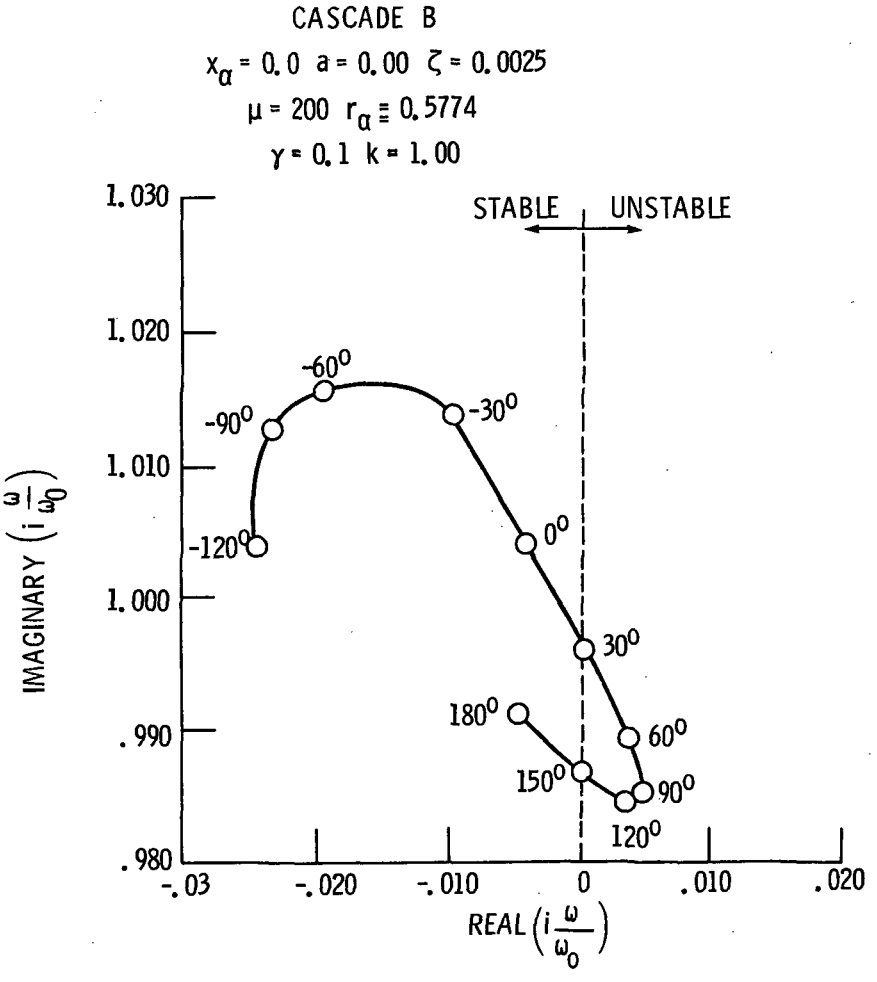

Figure 10. - Torsion mode root locus plot for a twelve bladed rotor.

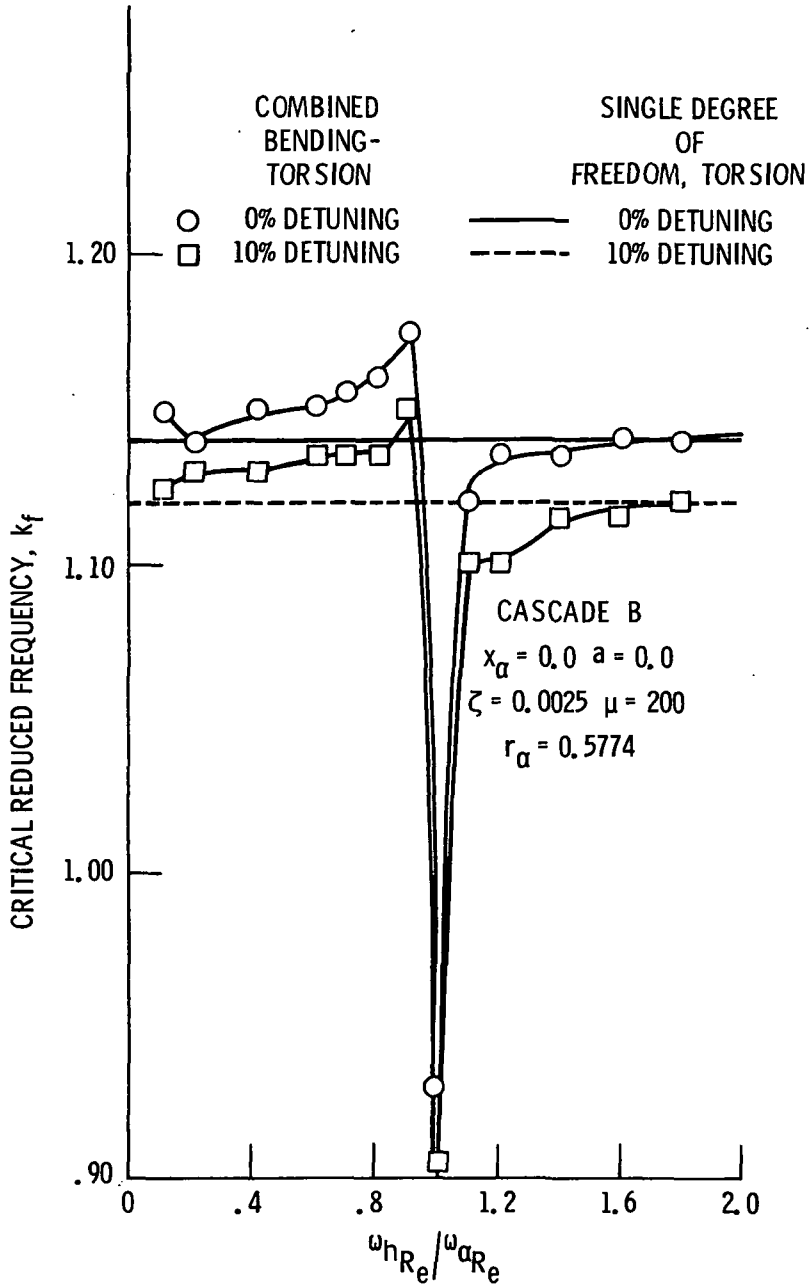

Figure 11. - The effect of aerodynamic detuning on the critical reduced frequency with a midchord elastic axis and center of gravity.

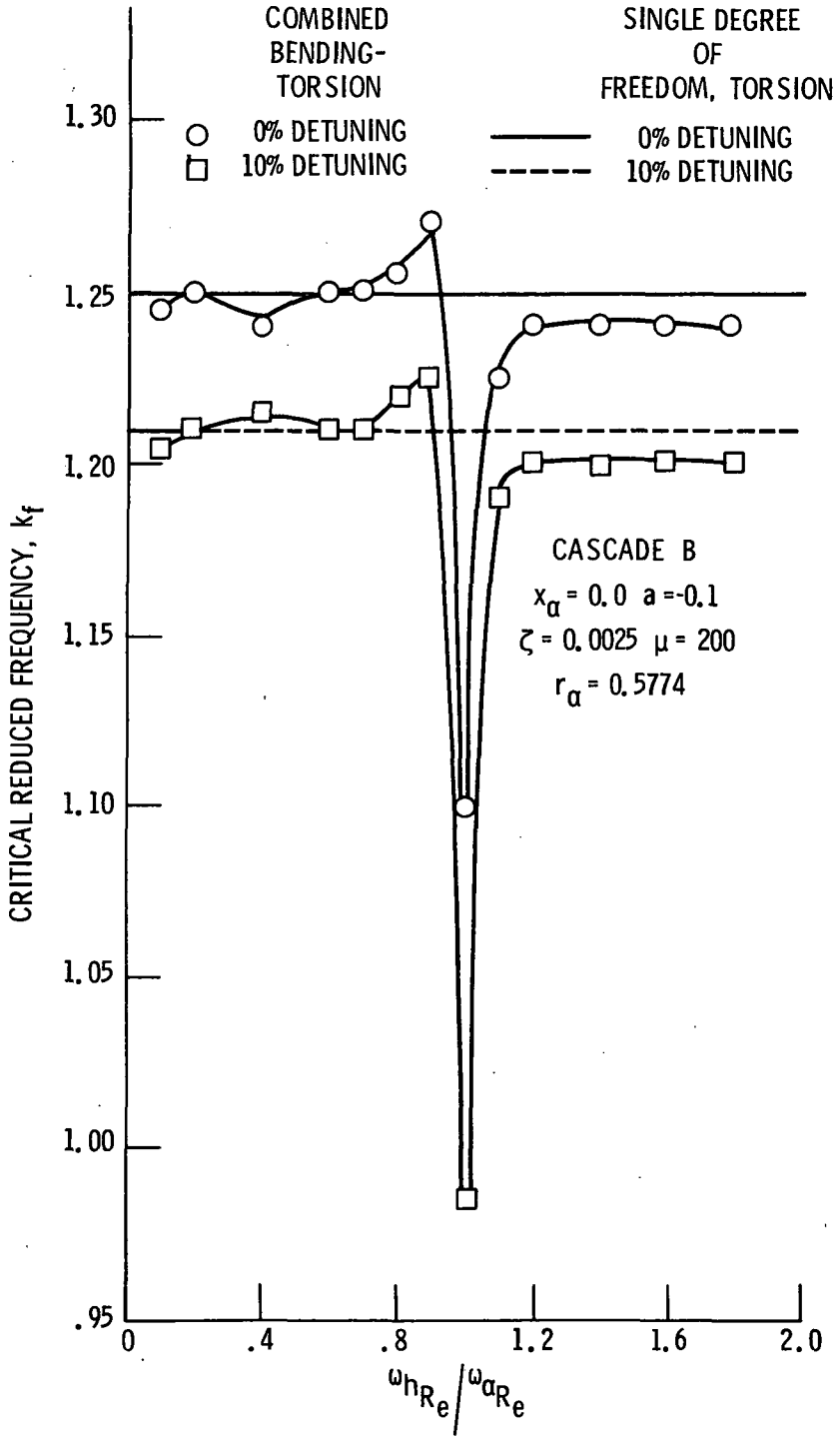

Figure 12. - The effect of aerodynamic detuning on the critical reduced frequency with the elastic axis and center of gravity located at 40% of the chord.

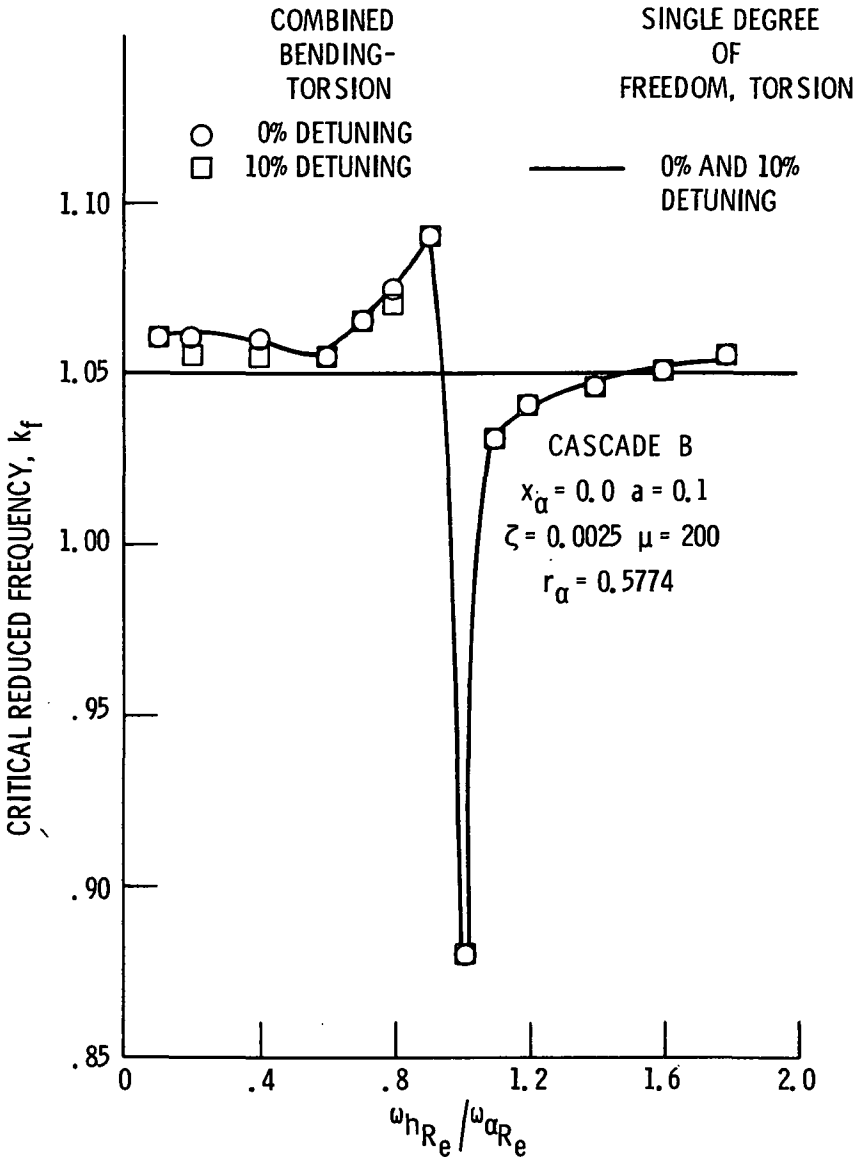

Figure 13. - The effect of aerodynamic detuning on the critical reduced frequency with the elastic axis and center of gravity located at 60% of the chord.

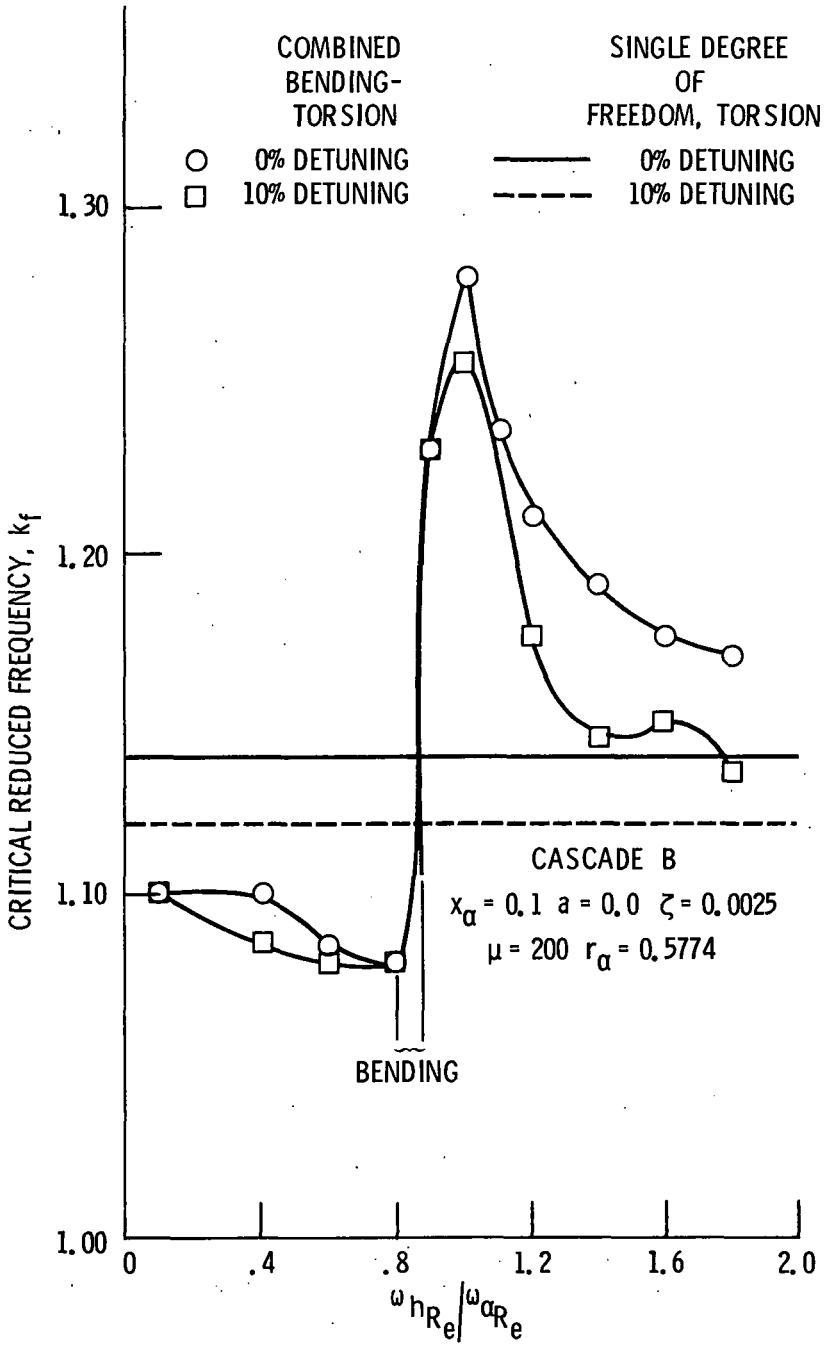

Figure 14. - The effect of aerodynamic detuning on the critical reduced frequency with the elastic axis at midchord and $X_\alpha = 0.1$.

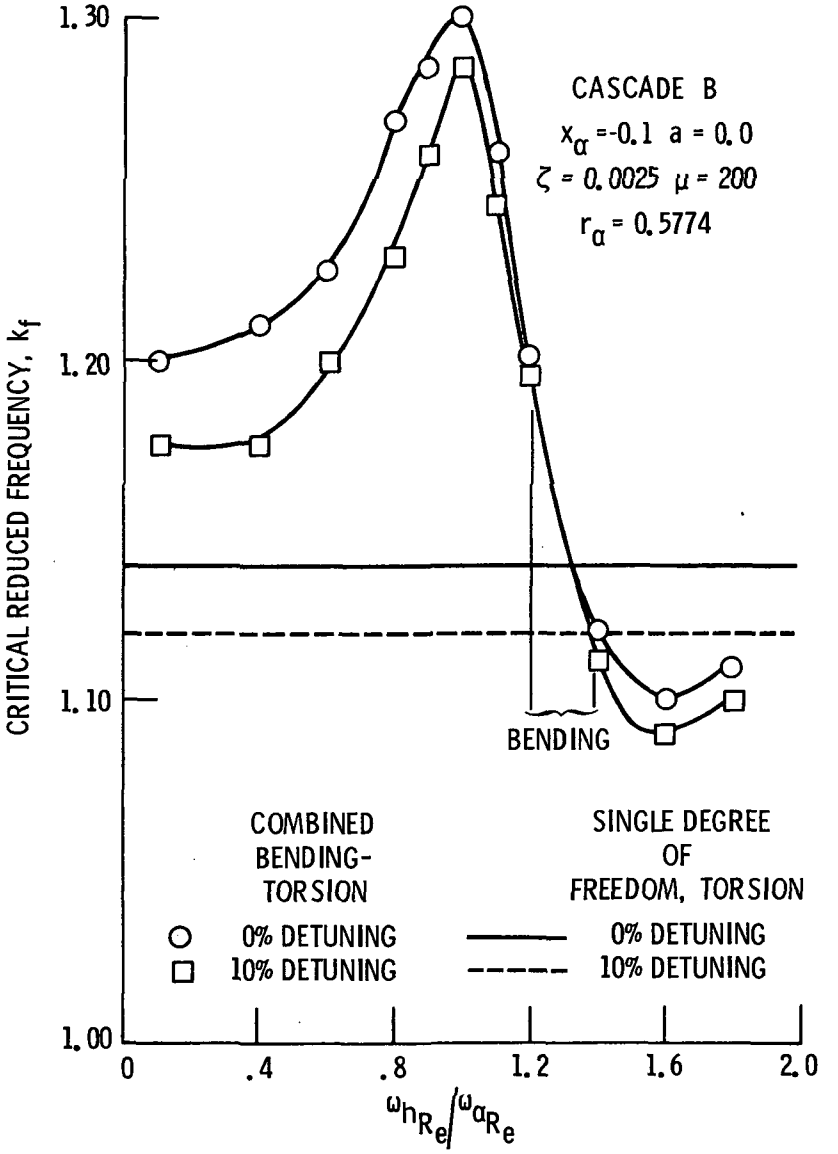

Figure 15. - The effect of aerodynamic detuning on the critical reduced frequency with the elastic axis at midchord and X_α = -0.1.

1. Report No.	2. Government Accession No.	3. Recipient's Catalog No.
NASA TM-87240		

4. Title and Subtitle	5. Report Date
The Predicted Effect of Aerodynamic Detuning on Coupled Bending-Torsion Unstalled Supersonic Flutter	6. Performing Organization Code 535-03-01
7. Author(s) Daniel Hoyniak and Sanford Fleeter	8. Performing Organization Report No. E-2915
	10. Work Unit No.
9. Performing Organization Name and Address National Aeronautics and Space Administration Lewis Research Center Cleveland, Ohio 44135	11. Contract or Grant No.
	13. Type of Report and Period Covered Technical Memorandum
12. Sponsoring Agency Name and Address National Aeronautics and Space Administration Washington, D.C. 20546	14. Sponsoring Agency Code

15. Supplementary Notes

Prepared for the 31st International Gas Turbine Conference sponsored by the American Society of Mechanical Engineers, Dusseldorf, West Germany, June 8-12, 1986. Daniel Hoyniak, NASA Lewis Research Center; Sanford Fleeter, Purdue University, School of Mechanical Engineering, West Lafayette, Indiana 47907.

16. Abstract

A mathematical model is developed to predict the enhanced coupled bending-torsion unstalled supersonic flutter stability due to alternate circumferential spacing aerodynamic detuning of a turbomachine rotor. The translational and torsional unsteady aerodynamic coefficients are developed in terms of influence coefficients, with the coupled bending-torsion stability analysis developed by considering the coupled equations of motion together with the unsteady aerodynamic loading. The effect of this aerodynamic detuning on coupled bending-torsion unstalled supersonic flutter as well as the verification of the modeling are then demonstrated by considering an unstable 12 bladed rotor, with Verdon's uniformly spaced Cascade B flow geometry as a baseline. It was found that with the elastic axis and center of gravity at or forward of the airfoil midchord, 10 percent aerodynamic detuning results in a lower critical reduced frequency value as compared to the baseline rotor, thereby demonstrating the aerodynamic detuning stability enhancement. However, with the elastic axis and center of gravity at 60 percent of the chord, this type of aerodynamic detuning has a minimal effect on stability. For both uniform and nonuniform circumferentially spaced rotors, a single degree of freedom torsion mode analysis was shown to be appropriate for values of the bending-torsion natural frequency ratio lower than 0.6 and higher than 1.2. However, for values of this natural frequency ratio between 0.6 and 1.2, a coupled flutter stability analysis is required. When the elastic axis and center of gravity are not coincident, the effect of detuning on cascade stability was found to be very sensitive to the location of the center of gravity with respect to the elastic axis. In addition, it was determined that when the center of gravity was forward of an elastic axis located at midchord, a single degree of freedom torsion model did not accurately predict cascade stability.

17. Key Words (Suggested by Author(s))	18. Distribution Statement
Flutter; Coupled bending-torsion; Cascade; Aerodynamic detuning	Unclassified - unlimited STAR Category 02

19. Security Classif. (of this report)	20. Security Classif. (of this page)	21. No. of pages	22. Price*
Unclassified	Unclassified		

*For sale by the National Technical Information Service, Springfield, Virginia 22161